



Published in final edited form as:

Magn Reson Med. 2013 March 1; 69(3): 862–867. doi:10.1002/mrm.24307.

On shimming approaches in 3T breast MRI

Ileana Hancu, PhD¹, Ambey Govenkar, MS², Robert E. Lenkinski, PhD³, and Seung-Kyun Lee, PhD¹

¹GE Global Research Center, Niskayuna, NY, USA

²Extenprise Inc, Pune, India

³UT Southwestern Medical Center, Dallas, TX, USA

Abstract

A comparative study is presented, analyzing quantitatively the impact of fifteen shim strategies on the homogeneity of the main magnetic field over the three dimensional breast region in 3T MRI. The results obtained in twelve female volunteers, spanning a wide range of body and breast types, indicate that the inclusion of the back and heart in the shim region of interest (ROI) leads to considerable decrease in the field homogeneity, and needs to be avoided. Comparison between shim strategies using volumetric B_0 maps, covering the entire breast region, and 1–6 plane B_0 maps indicate only minimally reduced performance for the latter. Interestingly, however, no single shim strategy relying on a limited number of B_0 maps as input was found to work best in all volunteers. This was attributed to the limited capability of a small number of B_0 maps to capture the B_0 variability existent within breast. On the average, a rectangular shim ROI, encompassing the breast region alone, worked best for the cohort studied here.

Keywords

breast; MRI; shimming; 3T; B_0

Introduction

Due to its very high sensitivity to detect cancer, breast MRI is becoming increasingly common (1,2). A slow transition of breast exams from 1.5T to 3T is also occurring (3). The additional challenges when imaging at high field, however, become particularly problematic for anatomies spanning large fields of view (FOV), and need to be mitigated to fully benefit from the higher field strength. In particular, signal loss, poor fat suppression, image blurring and image distortion have all been blamed on imperfect magnetic field homogeneity in 3T breast imaging exams (4). It is therefore important to understand the B_0 distribution over the 3-dimensional breast volume in a population of subjects, and develop shimming approaches that result in a homogeneous static field in such population.

While relatively limited attention has been paid to this topic up to now, understanding exists with respect to the presence of an inhomogeneous B_0 field over the breast region, and means to address it have been proposed. Solutions to improve the quality of the B_0 field for bilateral breast imaging include the use of dual shim regions of interest (ROI's) (5), further to be enhanced by spectral-spatial excitation of the two breasts, with individual shim values and center frequencies tailored for each of the two breasts (6). A single comprehensive

study, using electromagnetic simulations computing the B_0 field in a single volunteer and single slice B_0 acquisitions in a limited number of subjects, offers useful insights into the B_0 characteristics of the breast and means to improve the field homogeneity over this region (7). It was concluded in this study that a predominant linear gradient exists along the anterior-posterior axis of the breast, which is best shimmed by linear shims and saturation pulses (7).

Our work further expands this previous study, by examining three dimensional B_0 data sets collected from the breast region in a relatively large number of volunteers. Fifteen shim strategies, based on either 3D B_0 data, or 1–6 planes of B_0 data (sub-sampled from the initial data sets) are considered. Quantitative conclusions are drawn with respect to the advantages and disadvantages of using a given shim strategy, on an individual and on a populations basis.

Methods

In vivo experiments

Twelve female volunteers were scanned in a 3T, GE Discovery MR750 scanner (Waukesha, WI), following a protocol approved by our Institutional Review Board. The volunteers spanned a diverse range, with their height varying between 5ft 2in and 6ft 2in, their weight between 120 and 190lbs, and their body mass index between 21 and 31. Breast composition varied from almost entirely fat to almost entirely glandular tissue among these volunteers. The patients, who had no metallic implant or objects in their bodies, wore extra large t-shirts for the scans, which preserved the anatomy. They were scanned in the prone position, using a table-top, 8 channel GE breast coil. A three-plane localizer was followed by the acquisition of 32 slices of B_0 maps, in an axial orientation, at 3mm in plane and 6mm out of plane spatial resolution. The acquisition lasted 60 seconds. A 3-echo IDEAL algorithm (8) was used to reconstruct water, fat and B_0 maps. These maps, or subsets of these maps were used to shim offline; as high order shims were previously shown to add little benefit to breast imaging (5,7), only adjustment of linear gradients was considered here. Fifteen strategies were used for shimming, as shown in Figure 1. In this figure, the arrows in some of the strategies (2, 4, 6, 7, 9, 11, 13 and 15) indicate a multi-plane shimming approach, with the arrow highlighting the location of the B_0 planes (selected or re-sampled out of the initial volume of acquired B_0 maps) that were used as input for the shimming algorithm. Similar to the clinical approach, all multi-plane strategies rely on shimming in 3 orthogonal planes, chosen, by default, in the middle of the shim ROI chosen by the user. In practice, for some of the strategies, due to limited or no signal in these planes, the 3 planes can get reduced to 2 planes (strategy 7, with the sagittal plane being sometimes omitted, or in some volunteers, strategy 4), or 1 plane (strategy 6, where both the sagittal and coronal plane have minimal or no signal). In all other cases considered (strategies 1, 3, 5, 8, 10, 12 and 14), shimming was performed using all 28–32 slices of B_0 data (for subjects with smaller breasts, the number of slices was reduced from 32 to 28), masked by the rectangles visible in Figure 1. The figure of merit for the performance of the shim strategy was chosen to be the standard deviation of the B_0 maps after shimming, computed over all 28–32 B_0 planes below a horizontal line drawn just anterior to the heart (this corresponds approximately to the area enclosed in the rectangular prism shown in Figure 1, strategy 5).

For each of the last two volunteers, two additional series were added to the MR exam, to assess the performance of the multi-plane shim strategy deemed optimal by the analysis of data in the first ten volunteers. In these last two subjects, a short echo time, 3D fast gradient echo acquisition was performed, at 1mm isotropic resolution, taking 1 min of acquisition time. This is the typical sequence used for dynamic contrast enhanced (DCE) MRI acquisitions; it has little geometric distortion, therefore properly defines the subject's

anatomy. Subsequently, a diffusion weighted imaging (DWI) acquisition was performed, due to its high sensitivity to B_0 inhomogeneities. This sequence employed a double spin echo, echo-planar based readout, at 3mm through plane and 1.8mm in plane spatial resolution. The alignment between the DWI and the DCE images was examined, to assess the need to further refine the shim strategy, or to evaluate whether a post-processing correction is still needed for easy interpretation of the DWI images.

Results

Figure 2 shows an example of an average weight volunteer shimmed using 3 different shim scenarios. Figure 2a displays the result of shimming over the entire FOV, using volumetric B_0 maps (strategy 1). As previously observed (7), there is a strong anterior/posterior gradient over the breasts. This results in poor shimming over the breast region, should the entire axial FOV be included in the shim ROI. Figure 2b presents the result of shimming solely over the breast region, using volumetric B_0 maps (strategy 5). As it will be later discussed, this represents the best case scenario for breast shimming in our study. Note that the anterior/posterior gradient is now compensated by the shim gradients, at the expense of significantly increasing the resonant frequency of the subject's back. Figure 2c displays the results of shimming solely over the breast region, using a rectangular shim ROI, with only 3 orthogonal planes of B_0 data as input (strategy 7); as discussed in the next paragraph, this represents the best approach for shimming with a limited number of planes of B_0 data as input.

Table 1 contains an explicit description of the shim cases considered (2nd column). In addition, the third column of Table 1 displays the average B_0 standard deviation for each shim strategy; to obtain this quantity, the standard deviation of the B_0 field after shimming is computed for each volunteer below a line anterior to the heart; the average of the 12 standard deviations (one for each volunteer) is displayed for all shim strategies considered (3rd column). For ease of assessment, a ranking of the 15 shim strategies, based on the average standard deviation displayed in the 3rd column, is also presented in the 4th column of Table 1. Note a few very interesting facts emerging from this table:

- The heart and the back of the subjects need to be excluded from the shim ROI; among the 15 strategies considered, the only 4 including this information-- with multi-plane or volumetric B_0 data used as input-- rank last (strategies 1, 2, 3 and 4). This is due to the strong anterior/posterior gradient existent across the breasts, which significantly shifts their average resonance frequency away from the average resonant frequency of the body.
- The best shim strategy relies on volumetric B_0 data, and shims only over the breast region (strategy 5). Although somewhat impractical due to the long time needed for acquisition of the volumetric B_0 data, this approach is in fact the best for each of the subjects included in this study (data not shown).
- Among the multiple-plane strategies, strategy 7 (3 plane rectangular shim), 13 (6 plane square shim) and 6 (1 plane axial shim) represent the best alternatives to shimming using volumetric B_0 data as input. As evident from Figure 2, the difference between strategy 5 (best case scenario) and strategy 7 (best multi-plane scenario) is somewhat limited (8%, on the average, higher standard deviation in the multi-plane scenario of strategy 7 compared to the volumetric approach of strategy 5). Interestingly, however, there is no single multi-plane shim scenario that works best in all volunteers. Table 2 presents a detailed ranking of all multi-plane shim strategies for all 12 volunteers considered; the data in this table is obtained by assigning the value 7 to the shim strategy with the lowest standard deviation, 6 for

the second lowest, 5 for the third lowest, etc. The worst shim strategy had the value 0 assigned to it; in case two strategies were equivalent, producing equal standard deviations, the average of two rankings was assigned equally (e.g. volunteers 8 and 12). Note in this table, that although strategy 7 works well on the average, it works less well for volunteers 7, 9 and 10. This is due to the fact that intra-breast B_0 variability may exist, that is not captured well by the limited information existent in the multi-plane B_0 maps used in the non-volumetric shim strategies.

- Although avoiding the chest wall or nipple area is sometimes recommended for breast shimming, better overall results are obtained when these areas are included the shim ROI's (note in Table 1 that strategy 12 ranks higher than 14, and 13 ranks higher than 15). Although improved B_0 homogeneity can be seen in some subjects when excluding the nipple and chest wall areas from the shim ROI's (e.g. volunteers 1, 2, 4 and 11 in our study (Table 2)), the inclusion of these areas in the shim ROI's results in better results in a cohort of subjects.

Figure 3 presents the average field for the right and left breasts (after shimming using strategy 5) as a function of slice number for two of the 12 volunteers studied. These two volunteers are representative of the two types of behaviors we have observed: in some of the volunteers (3/12) the right and left breast have opposite through-slice behaviors, while in the others (9/12), the two breasts have similar through-slice behaviors. This finding points to the fact that, besides breast shape, general anatomy also determines the B_0 distribution; the breasts of none of the volunteers were touching the coil surface, which could have disturbed the half-sphere shape differently on the right and left side of the body.

Figure 4 presents an overlap between the anatomical image and the DWI image (one slice) acquired in one of the last two volunteers, using the best multi-plane shim strategy (strategy 7). Note the very good overlap over the breast region between the fine details evident both in the anatomical and DWI image (pink arrow). Overall, it is estimated that most pixels in the breast region of the DWI image would need less than 1 pixel shift to perfectly align them with their counterparts in the anatomical image.

Discussion and conclusions

A population study was conducted, investigating the best approach for shimming the breast region in 3T MRI exams. Seven shim strategies based on volumetric B_0 data as input, and eight shim strategies based on 1–6 planes of input B_0 data were considered in our study. While some of the qualitative results of this study are intuitive (e.g. shimming over the breast region using volumetric B_0 data yields best overall field homogeneity), some are less obvious and provide quantitative answers with respect to what is the impact of shim strategy on breast field homogeneity.

It was concluded at the end of our study that the heart and the back of the subjects should never be included in the shim ROI's for breast exams. The imperfect B_0 field uniformity in the subjects' cross section (Figure 2) is due to two factors. First, the dipolar fields created by the spins existent in each voxel of the diamagnetic tissue add/subtract to the homogeneous field created by the magnet, and result in a strong anterior/posterior gradient over the breast region (7). Secondly, most breast exams are performed using table-top breast coils, which place the breast region in the center of the magnet. Consequently, the back/shoulders of the subjects can extend beyond the region of scanner field homogeneity, and result in significant changes in magnetic field in these anatomical regions (note the “hot” shoulder/back of the volunteer in Figure 2a). While this should be in fact inconsequential, as no data is desired from the back of the subject when a breast exam is performed, the inclusion of such regions for the shim part of prescan result, on the average, in a 35–80% drop in B_0 uniformity (Table

1). Note, however, that creating a well-shimmed and on-resonance breast region significantly increases the frequency of the subjects' back (Figure 2b and 2c); the average resonant frequency of the subjects' back, computed over a region posterior to the heart, was 484 (± 110) Hz higher than the average frequency of the breasts. Depending on the readout sequence or sequence parameters used, this may result in signal wraparound or aliasing, and may require spatial pre-saturation pulses (properly offset in frequency) to circumvent this issue.

Although we have not specifically quantified the performance of the shim strategies in the axillae, some insights can be gained by visual inspection of the B_0 maps after shimming. After applying the y gradients that compensate for the strong anterior-posterior gradient over the breasts, the axillae tend to resonate at frequencies similar to the breasts' and lower than the heart's or liver's (Figure 2b). Consequently, extended shim ROI's, that include the heart/liver areas (e.g. strategies 1/2/3/4), perform worse in the axillae than strategies that avoid them. The best approaches to improve field homogeneity over the breast area (strategies 5/7 and 12/13) also seem to offer the best results for the axillae. A tailored shim ROI that would purposely select the breasts and the axillae, while excluding the heart/liver (of a crescent moon type shape, e.g.), would probably yield better overall results, yet be more difficult to prescribe in typical clinical situations.

It was also found in our study that no single multi-plane strategy works best for all individuals studied (Table 2); the intra-breast B_0 variability, cannot be captured well by a limited number of B_0 planes. Consequently, comparisons between shim strategies or image quality should be performed on a cohort, and not on an individual basis. This conclusion should also be reached by a quick examination of Figure 3. In addition to breast shape, other factors, such as body type or position of internal organs, influence the B_0 distribution over the 3 dimensional volume of the breast. A shimming strategy that alternates shim values to best accommodate each breast (6) may make little difference in a volunteer such as the one displayed at the bottom of Figure 3; in this case, both breasts exhibit very similar behavior. The same approach, however, may improve shimming in a volunteer such as the one displayed at the top of Figure 3; for such a subject the right and left breasts exhibit considerably different behavior.

This study offers insight into the improvements that can be obtained by moving from a multi-plane to a volumetric shim strategy-- at the expense of increasing the acquisition time for B_0 maps. With static shims, a 8% reduction in the B_0 standard deviation is obtained going from the best volumetric approach (strategy 5) to the best 3 plane shim approach (strategy 7) (Table 1). It is therefore suggested that multi-plane shim strategies may be adequate for the majority of breast exams. In particular, a rectangular shim ROI (strategy 7) or double cuboid ROI's, encompassing both the chest wall and the nipple areas (strategy 13), yields best results in a population of subjects. For the exams particularly sensitive to B_0 inhomogeneities, such as DWI, fast B_0 mapping strategies, such as the ones described in (9,10), coupled to dynamic shimming (per-slice (11) or per slab (6) shim and center frequency adjustment), may result in better overall image quality.

Acknowledgments

Grant support: 1R01CA154433

References

1. Bleicher RJ, Morrow M. MRI and breast cancer: role in detection, diagnosis, and staging. *Oncology* (Williston Park). 2007; 21(12):1521–1528. 1530. discussion 1530, 1532–1523. [PubMed: 18077995]

2. Turnbull L. Dynamic contrast-enhanced MRI in the diagnosis and management of breast cancer. *NMR Biomed.* 2007; 22:28–39. [PubMed: 18654999]
3. Meeuwis C, Mann RM, Mus RD, Winkel A, Boetes C, Barentsz JO, Veltman J. MRI-guided breast biopsy at 3T using a dedicated large core biopsy set: feasibility and initial results. *Eur J Radiol.* 2011; 79(2):257–261. [PubMed: 20541338]
4. Harvey JA, Hendrick RE, Coll JM, Nicholson BT, Burkholder BT, Cohen MA. Breast MR imaging artifacts: how to recognize and fix them. *Radiographics.* 2007; 27 (Suppl 1):S131–145. [PubMed: 18180223]
5. Kim D, Spielman D, Daniel B. Automated bilateral shimming for breast MRI. 2002:636.
6. Han, M.; Rodriguez, S.; Sawyer, A.; Daniel, B.; Cunningham, C.; Pauly, J.; Hargreaves, B. Fat suppression with independent shims for bilateral breast MRI. Honolulu, Hawai'i: 2009. p. 580
7. Maril N, Collins CM, Greenman RL, Lenkinski RE. Strategies for shimming the breast. *Magn Reson Med.* 2005; 54(5):1139–1145. [PubMed: 16217775]
8. Reeder SB, Pineda AR, Wen Z, Shimakawa A, Yu H, Brittain JH, Gold GE, Beaulieu CH, Pelc NJ. Iterative decomposition of water and fat with echo asymmetry and least-squares estimation (IDEAL): application with fast spin-echo imaging. *Magn Reson Med.* 2005; 54(3):636–644. [PubMed: 16092103]
9. Chang H, Fitzpatrick JM. A technique for accurate magnetic resonance imaging in the presence of field inhomogeneities. *IEEE Trans Med Imaging.* 1992; 11(3):319–329. [PubMed: 18222873]
10. Roopchansingh V, Cox RW, Jesmanowicz A, Ward BD, Hyde JS. Single-shot magnetic field mapping embedded in echo-planar time-course imaging. *Magn Reson Med.* 2003; 50(4):839–843. [PubMed: 14523971]
11. Morrell G, Spielman D. Dynamic shimming for multi-slice magnetic resonance imaging. *Magn Reson Med.* 1997; 38(3):477–483. [PubMed: 9339449]

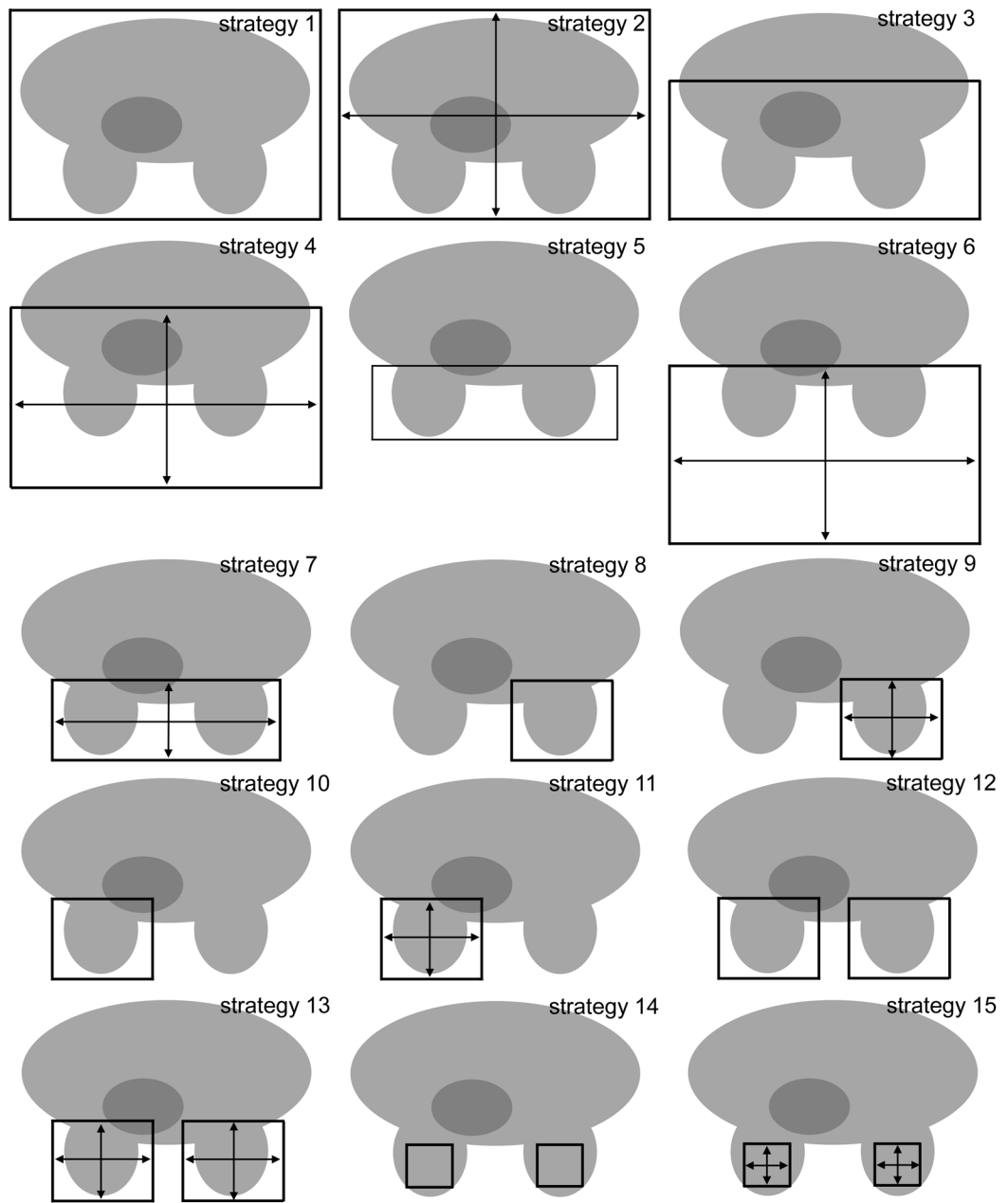


Figure 1. Graphical illustration of the 15 shim strategies considered. The rectangles define the regions over which shimming was performed; the arrows existent in some cases indicate the location of the perpendicular planes used for shimming.

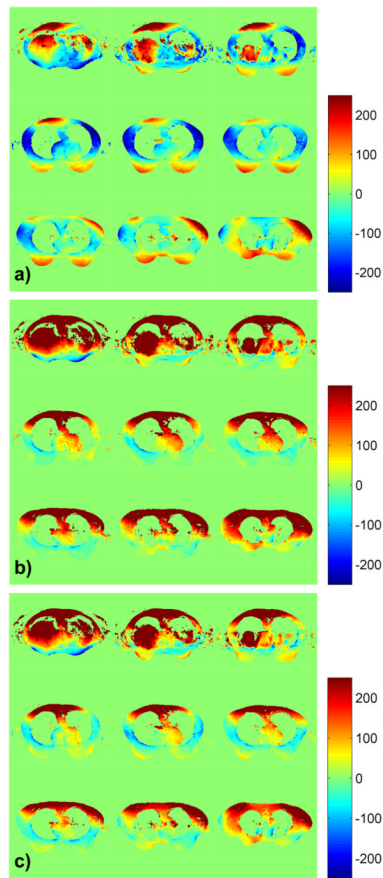


Figure 2. B_0 maps from a normal volunteer, after shimming using **a)** strategy 1 **b)** strategy 5 and **c)** strategy 7.

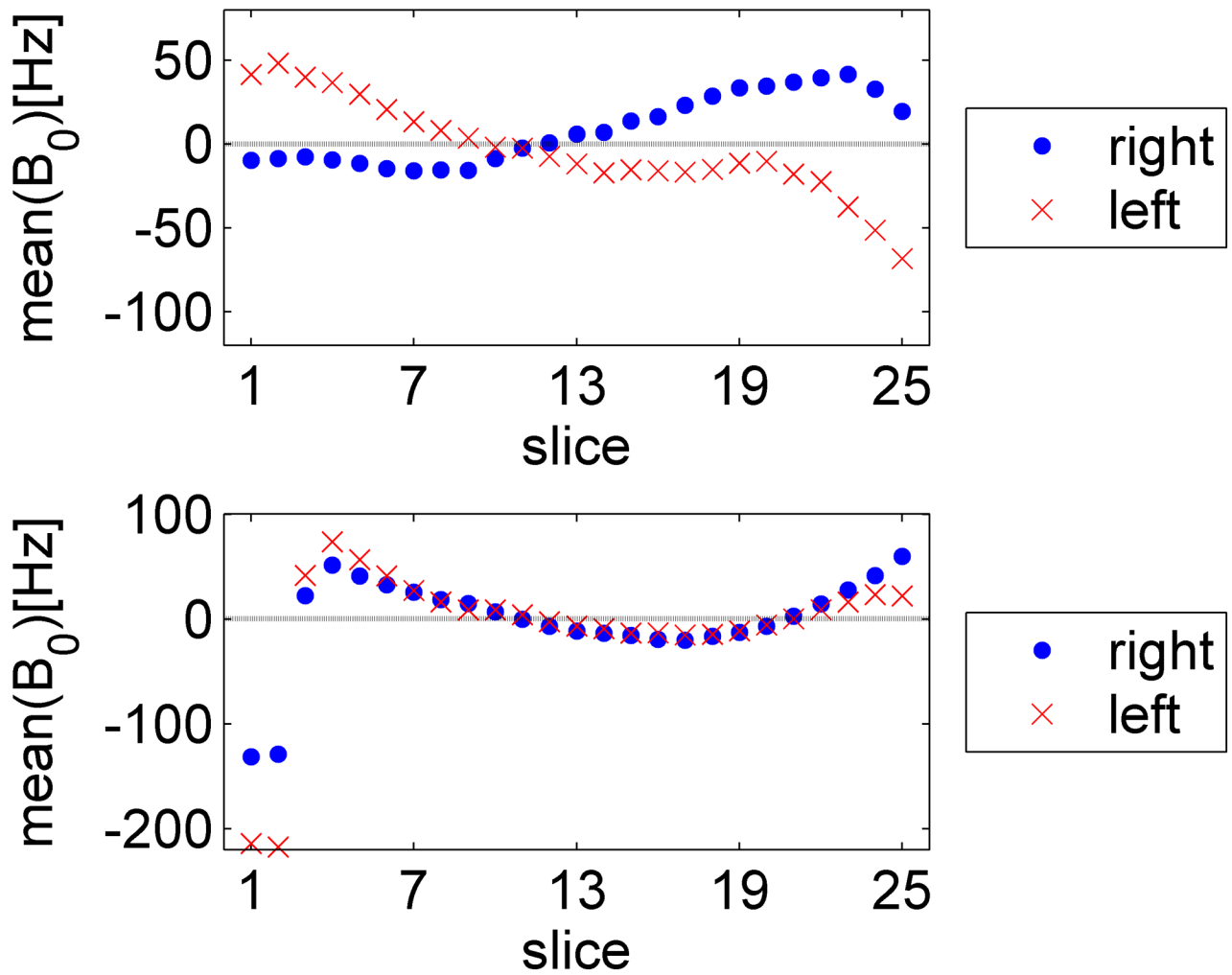


Figure 3. Average field in the right (dots) and left (crosses) breast as a function of (axial) slice number, following shimming using strategy 5. Two volunteers, illustrating the two separate trends we have observed in our cohort of subjects, are displayed (top and bottom).

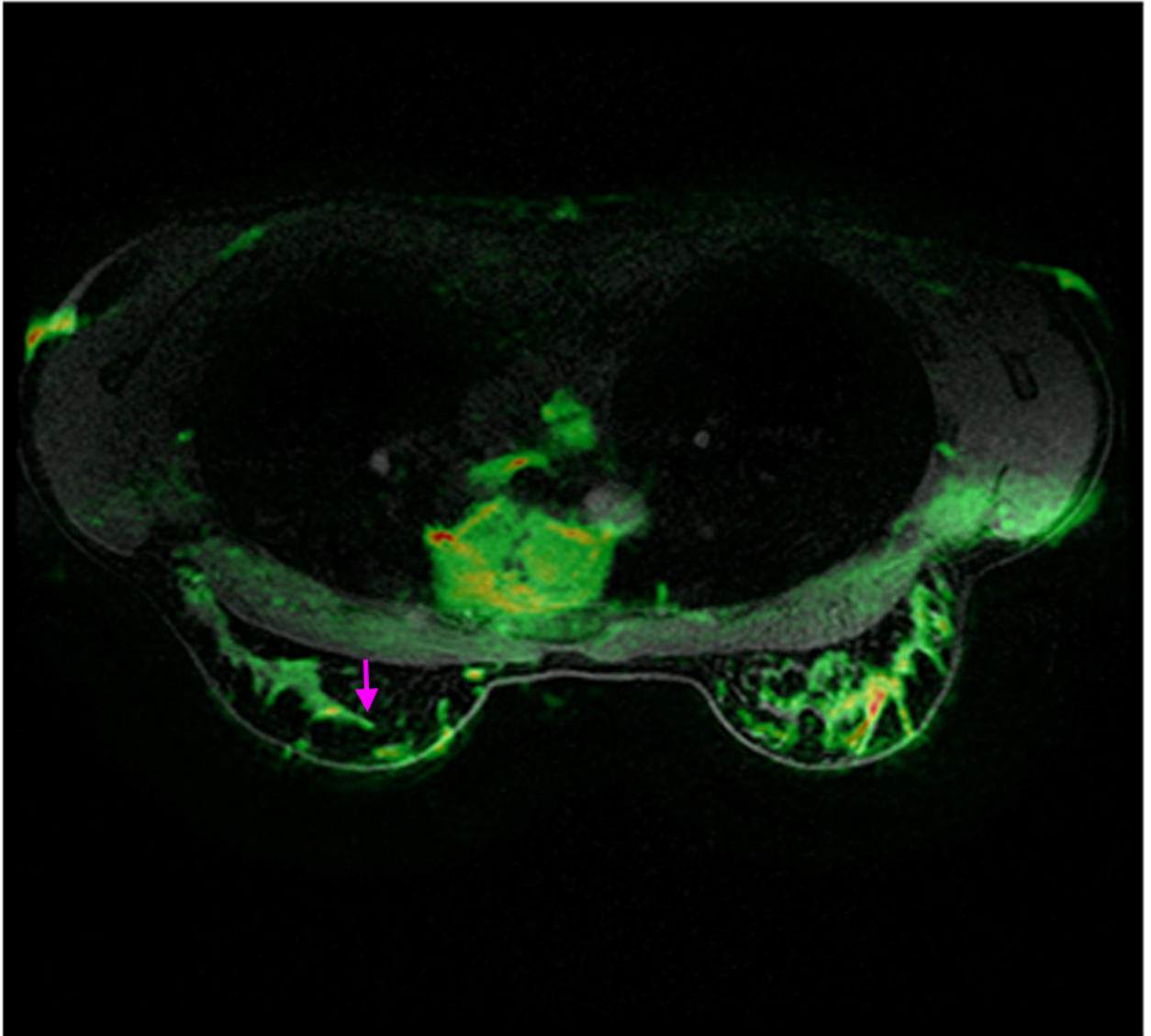


Figure 4. Mid-slice from a normal volunteer, with the anatomical and DWI images overlapped. The volunteer was shimmed using the best multi-plane shim strategy (strategy 7). Note the good match between the fine details of the two images (pink arrow).

Table 1

Summary of the shim strategies considered, the average standard deviation in all 12 volunteers for each shim strategy, and the overall ranking of the shim strategies.

Shim strategy	Description	Std (Bo)	Shim rank
1	3D shim over the entire FOV	70.9	15
2	3 plane shim over the entire FOV	68	14
3	3D shim avoiding the back, but including the heart	52.6	12
4	3 (or 2) plane shim avoiding the back, but including the heart	54.6	13
5	3D shim over the breasts	35.8	1
6	1 plane (axial only) shim over the breasts	41.6	7
7	3 plane rectangular shim over the breasts	38.9	3
8	3D shim over the right breast	39	4
9	3 plane shim over the right breast	51	11
10	3D shim over the left breast	40.8	6
11	3 plane shim over the left breast	46.3	10
12	average 3D shim over the 2 breasts	37.1	2
13	6 plane shim over the 2 breasts	42.3	8
14	average 3D shim over cuboid ROI's inside each breast that avoid the chest wall and nipple area	39.1	5
15	6 plane shim over cuboid ROI's inside each breast that avoid the chest wall and nipple area	42.8	9

Table 2

Performance of the multi-plane shim strategies in all individual volunteers.

	Strategy 2	Strategy 4	Strategy 6	Strategy 7	Strategy 9	Strategy 11	Strategy 13	Strategy 15
vol 1	3	6	5	7	0	4	1	2
vol 2	0	2	7	6	1	3	4	5
vol 3	0	2	7	6	1	3	5	4
vol 4	1	0	5	6	2	7	3	4
vol 5	1	2	6	7	3	0	5	4
vol 6	1	0	2	7	3	5	6	4
vol 7	0	1	3	5	2	4	7	6
vol 8	0	4	2	6.5	6.5	1	5	3
vol 9	0	2	5	4	1	7	6	3
vol 10	0	1	3	5	4	7	6	2
vol 11	0	2	5	7	1	6	3	4
vol 12	0	1	4	6.5	2	3	6.5	5
Total	8	26	60	80	30.5	51	62.5	46
Stdev	1.0	1.6	1.7	1.0	1.7	2.4	1.7	1.2